Measurement of Interfacial Toughness
in Thermal Barrier Coating Systems by Indentation

M. J. Stiger, L. A. Ortman, F. S. Pettit and G. H. Meier
Department of Materials Science and Engineering
University of Pittsburgh

R. Handoko, A. Vasinonta and J. Beuth
Department of Materials Science and Engineering
Carnegie Mellon University

Introduction

Ceramic thermal barrier coatings (TBCs) are currently used to insulate gas turbine components. However, a major concern with TBCs is their loss of adhesion during service, leading to spallation. Adhesion loss is related to oxidation occurring between the TBC and substrate. The goal of the work described in this paper is to use indentation tests, microstructual observations and knowledge of oxidation mechanisms to: quantify losses in interfacial toughness with thermal exposure, identify mechanisms for apparent toughness loss, separate contributions to toughness resulting from each mechanism and develop an accelerated testing technique for TBC failure.
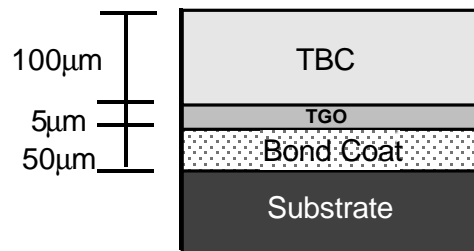

Figure 1. Diagram of a Typical Thermal Barrier Coating System

In this work, the size of the specimen studied is 1" diameter and 1/8" thick. Figure 1 shows a schematic diagram of a typical TBC system prepared by electron beam physical vapor deposition (EBPVD). The system consists of four layers, Ni superalloy substrate (N5), grit blasted Pt modified aluminide bond coat, thermally grown oxide (α-alumina) and yttria stabilized zirconia (YSZ) TBC. Selected area electron diffraction (SAD) and laser piezospectroscopy indicate the grit blasted bond coat develops an α-alumina TGO during TBC processing. Typical compressive stresses in the TGO and TBC are 3.5 GPa and 50 - 200 MPa respectively. The TGO is relatively thin but highly stressed.

Indentation Test

Figure 2 shows a schematic diagram of the indentation test being used to measure the interfacial toughness which is based on existing work for diamond films on Ti alloys [1]. A Rockwell Hardness tester is used to indent the specimens. The TBC and TGO are penetrated and plastic deformation is induced in bond coat and superalloy substrate. This plastic defromation results in radial displacements with axisymmetry about the indentor. Continuity is assumed across the interfaces, which results in compressive stresses in the TGO and TBC. The compressive radial stress drives the axisymmetric delamination and the radius of the debond is determined by the interfacial toughness. This test yields physical insight before fracture mechanics analysis is perfomed, e.g.

- Transition from no delamination from delamination
- Radius of delamination changes with exposure
- Can get buckling (Figure 3)
- Buckling complicates analysis to extract toughness, but transition to buckling gives added feedback on (assumed) compressive residual stress magnitudes

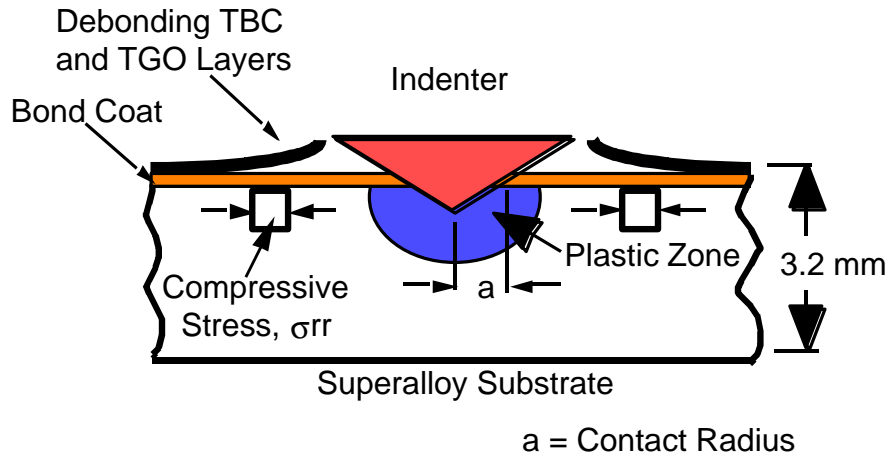- Buckling also makes visualization of delamination radius easier
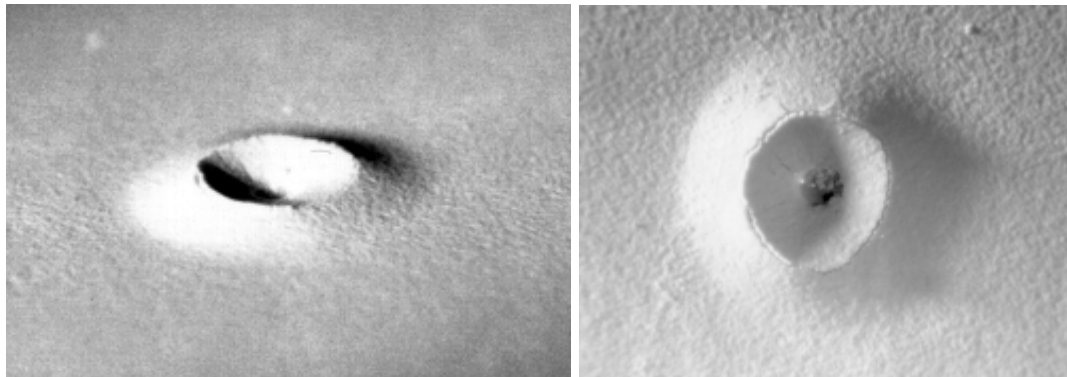

Figure 2. Diagram of the Indent Test

Figure 3. Photographs showing the surface of the TBC exposed 500h at 1100°C after indentation. The buckle diameter is 3.8mm.

Finite Element Modeling of the Indentation Problem

The indent test requires modeling of the deformation of a two-layered isotropic substrate. Finite element modeling (FEM) is used to quantify displacements of the bond coat and superalloy substrate. Modeling assumptions include the substrate has a one inch diameter geometry and the detailed shape of the brale indenter has a rounded tip instead of a sharp point. A cylindrical coordinate system is used with the origin placed at the center of the indent. Since a conical Brale indentor is used, Displacements are independent of theta. Figure 4 shows the two dimensional mesh for the TBC model from r=0", indent location, to r=0.5", the edge of the sample.
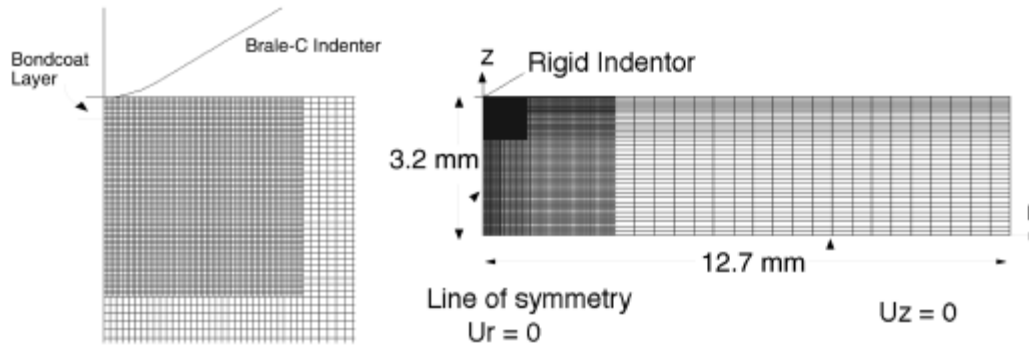
Figure 4. TBC modeling mesh

Tests to determine the effects of friction between the indenter were performed at multiple loads on the superalloy Rene '77. The change in contact radius is recorded, see Figure 5. It shows the friction coefficient considerably effects the numerical results of the modeling. Known properties from separate tensile tests of Rene '77 were applied as substrate properties in the model. Rene '77 was substituted for the real substrate-bond coat system for simplicity. The load versus contact radius results agree best with predictions of a coefficient of friction as 0.7. This coefficient of friction was then applied in subsequent modeling.
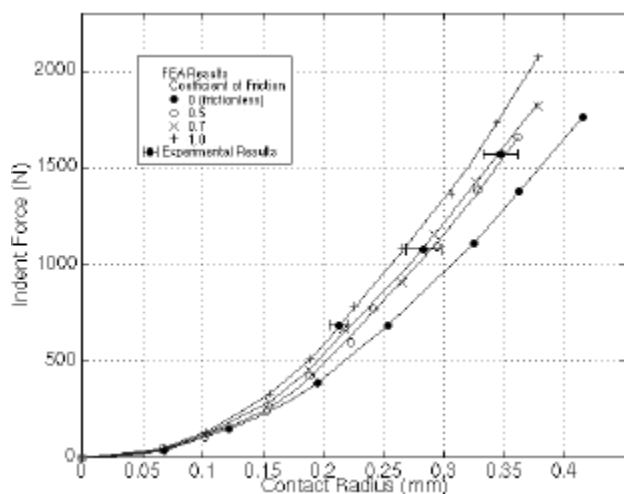

Figure 5. Results of the Current Model in Predicting Measured Load vs. Contact Radius Results for Indentation of Rene '77

Figure 6 compares the load vs. contact radius results of the indentation tests of the actual substrate with bond coat system to the model predictions. Both results agree well especially at high indent loads. In order to indicate the importance of some of the modeling assumptions, a simplified model using Drory and Hutchinson's assumptions, namely a sharp conical indenter and single material substrate having large dimensions, was used and the results are compared with the results from the current TBC model. At the same level of indent load, the contact radius from the model using simplified assumptions

is larger than that predicted by the current TBC model. The differences between the two numerical results come primarily from the friction contact condition added to the current model.
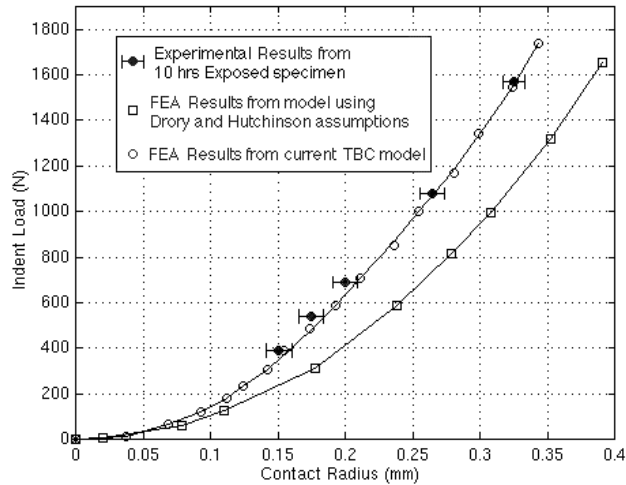

Figure 6. Results of the Current Model in Predicting Measured Load vs. Contact Radius Results for Indentation of a Bond Coat/N5 Superalloy Substrate

Figure 7 provides a comparison of the results from "TBC specimen" sized and "large substrate" models over a large range of R/a values. Several observations can be made by comparing the distribution of the radial displacement, Ur, in each case. First, for the TBC specimen sized model, indent load magnitudes affect the results when R/a is larger than approximately 5 and the plots show that larger applied loads produce larger displacements. To see the effect of substrate size, results are also presented from a model using identical conditions as the TBC specimen model except that the model size is changed to the large substrate size. By comparing the results from the standard size and large size models, it is clear that the size of the specimen considerably affects the results for large R/a. The radial displacement, Ur, from standard and large size TBC models agree well at small R/a but when R/a is larger than 5, the displacements from the standard size model decrease at a much slower rate than the large size model. The reason for this is that for R/a larger than 5, the radial displacements in the standard size model begin to experience free end effects from the specimen edge, which allow material to move more freely in the radial direction. In contrast, in the large size model radial displacements are resisted by the surrounding substrate.

For completeness, the results from the large substrate model using the simplified assumptions of Drory and Hutchinson (but using a flow theory of plasticity) are also compared in Figure 7. The displacements from the model with simplified assumptions are significantly lower than those from the TBC models except at very small R/a. Again, this is due primarily to neglecting friction.

Results obtained in this work allow an evaluation of the validity of assumptions made in large sample model in modeling TBC specimen indentation at the applied major loads available in a standard Rockwell hardness tester. Results presented in this paper and

other results generated in this work show that use of a sharp indenter and a deformation theory of plasticity will give essentially the same results as a model using a rounded indenter tip and a flow theory of plasticity. This is because applied major loads are large enough that the details of contact early in the indentation process (where tip geometry and non-proportional loading effects can significantly affect the results) are not important. A similar conclusion can be made concerning the role of the bond coat and bond coat properties. Applied major loads are large enough that the deformation of the superalloy substrate dominates the indentation problem. The exception to this is at locations R/a that are not substantially larger than the normalized bond coat thickness, t/a. At R/a values outside of these locations, (which are confined to values of R/a > 3), a single-layered substrate model is sufficient.
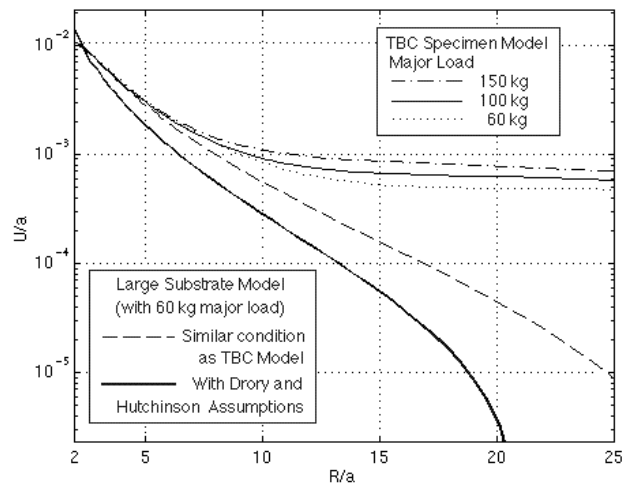

Figure 7. Plot of U/a vs. R/a for Three Load Values Obtainable in a Rockwell Hardness Tester

Important effects that must be included in modeling TBC indent specimens are those of specimen size and contact friction. Results given in this paper have demonstrated that contact friction can affect results significantly. Substrate size effects become very important for values of R/a greater than approximately 5. This also causes radial displacement results to be a function of the applied load for R/a > 5. It will be shown in the next section that delamination radius values in TBC systems are typically in this "large radius" regime.

The procedure for extracting an interfacial toughness from a numerical indentation model and the radius of delamination observed in an indent test is outlined by Drory and Hutchinson [1]. Only the essential equations will be repeated here. First, the total radial strain, ε_r, and circumferential strain, ε_θ, can be calculated by combining the biaxial residual strain, ε_o, with the strains caused by the indentation (calculated from the numerical model results). The relations can be written as

$$\varepsilon_\theta = \varepsilon_\theta^I + \varepsilon_o \quad (1)$$

and

$$\varepsilon_r = \varepsilon_r^I + \varepsilon_o \quad (2)$$

where

$$\varepsilon_\theta^I = \frac{U}{r} \quad (3)$$

and

$$\varepsilon_r^I = \frac{dU}{dr} \quad (4)$$

Here, the residual strain is calculated from the approximated residual stress. For the purpose of obtaining illustrative results, typical residual stress values reported in the literature for the TBC and TGO of 70 MPa [2] and 3.5 GPa [3,4] respectively will be assumed here. For the purposes of calculating the energy release rate due to debonding of the coating and oxide, an average residual in TBC/TGO layers can be used, defined as

$$\sigma_o = \frac{\sigma_{TBC}\ t_{TBC}\ + \sigma_{TGO}\ t_{TGO}}{t_{TBC}\ + t_{TGO}} \quad (5)$$

where t is the thickness of the TBC or TGO. An effective Young ' s Modulus for the uniform biaxial stress in TBC/TGO layers can also be defined as

$$\overline{E}_{eff} = \frac{\overline{E}_{TBC}\ t_{TBC}\ + \overline{E}_{TGO}\ t_{TGO}}{t_{TBC}\ + t_{TGO}} \quad (6)$$

where

$$\overline{E} = \frac{E}{1-\nu} \quad (7)$$

The residual stress can then be converted to a biaxial residual strain by using the relation

$$\varepsilon_o = \frac{\sigma_o}{E_{eff}} \quad (8)$$

The elastic properties of the TBC are estimated by the properties of MgO-PSZ (Partially Stabilized Zirconia) taken from [5] which are E = 200 GPa and $\nu = 0.22$. The elastic properties of TGO are estimated by the properties of α–Al$_2$O$_3$ (99.9%) from [6] which are E = 393 GPa and $\nu = 0.22$. The thicknesses of the TBC and TGO are taken as 100μm and 5μm, respectively, as designated in Figure 1. By substituting ε_r and ε_θ as a function of R/a into the relations,

$$\frac{2G(1-\nu)(1+\nu)}{E_{eff}\ t} \;=\; \left[\varepsilon_r\left(\frac{R}{a}\right)+\nu\varepsilon_\theta\left(\frac{R}{a}\right)\right]^2 \qquad (9)$$

and

$$\frac{2G(1-\nu)(1+\nu)}{E_{eff}\ t}=\left\{\varepsilon_r\left(\frac{R}{a}\right)+\nu\varepsilon_\theta\left(\frac{R}{a}\right)-\frac{(1-\nu^2)\,\varepsilon_\theta\left(\frac{R}{a}\right)\left[1-\left(\frac{R_i}{R}\right)^2\right]}{(1-\nu)+(1+\nu)\left(\frac{R_i}{R}\right)^2}\right\}^2 \qquad (10)$$

the distribution of energy release rate (G) for two extreme delamination process models namely, delamination leaving behind a very narrow annular plate of film and delamination with an unbuckled annular plate of film left behind the crack tip, can be obtained. R_i and R in equation 10 are the inner and outer radius of the crack respectively. Because it typically involves a buckling of the TBC, the distribution of energy release rate G from the TBC indentation should lie between these two distribution curves. It should be noted that E_{eff} is defined analogous to $\bar{E}_{eff}$ in the equation (7) but $\bar{E}$ is replaced by E instead.

Finally, the distribution of K vs. R/a for both delamination models which bracket the actual K can be calculated by using the relation

$$K \;=\; \sqrt{\frac{G\ \bar{E}_{TGO}\ (1-\alpha)}{1-\beta^2}} \qquad (11)$$

where

$$\alpha=\frac{\bar{E}_{TGO}-\bar{E}_{Bond\ Coat}}{\bar{E}_{TGO}+\bar{E}_{Bond\ Coat}}\ , \qquad (12)$$

and

$$\beta=\frac{\mu_{TGO}\,(\kappa_{Bond\ Coat}-1)-\mu_{Bond\ Coat}\,(\kappa_{TGO}-1)}{\mu_{TGO}\,(\kappa_{Bond\ Coat}+1)+\mu_{Bond\ Coat}\,(\kappa_{TGO}+1)} \qquad (13)$$

Here, for plane strain condition

$$\bar{E} = \frac{E}{1-v^2}, \quad (14)$$

$$\mu = \frac{E}{2(1+v)}, \quad (15)$$

and

$$\kappa = 3 - 4v \quad (16)$$

It should be noted that because the elastic properties used for the TBC/TGO and substrate/bond coat are assumed to be essentially the same, using the equation 11 for K is reasonable. The resulting distributions of K from both models are shown in Figure 8 for three different applied major loads, 60 kg, 100 kg and 150 kg obtainable in a Rockwell hardness tester. It is clear from Figure 8 that equation 9 and equation 10 can give substantially different Kc results. It is demonstrated in the next section, however, that even with these differences, insight can be gained into the loss of adhesion in TBC systems.
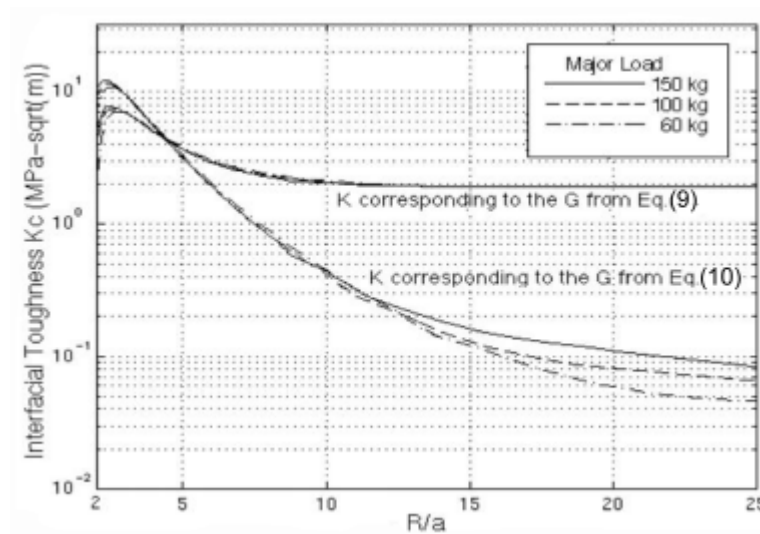

Figure 8. Plot of K vs. R/a for a TBC System with 3 Applied Major Loads and Assumed Residual Stress Levels in the Oxide and TBC

TOUGHNESS MEASUREMENTS

In this section, the methods and results outlined in the previous section are applied to the indentation of TBC specimens consisting of an N5 single crystal substrate, a chemical vapor deposited PtAl bond coat, a TGO, and an EBPVD yttria stabilized zirconia TBC. Specimens were subjected to various periods of exposure at 1200°C. In the indentation tests, a Rockwell hardness tester was used with brale C indenter, 150 kg major load and 10 kg minor load. The interfacial toughness can be obtained directly from Figure 8 by using the normalized delamination radius R/a from the test to determine Kc. The

measured R/a from four indent tests and the corresponding Kc values obtained from Figure 8 are shown in Table 1. For the as-processed case, which experienced no debonding due to indentation, the maximum values of Kc corresponding to a value of R/a equal to 2.4 are taken as lower bounds on the interfacial toughness. Although the toughness values obtained from the two curves in Figure 8 are significantly different, both sets of results indicate that a significant decline in toughness occurs between exposure times of 0 and 10 and 10 and 20 hrs at 1200°C. Additional losses in toughness after 20 hours at 1200°C are small in magnitude. Multiple indentation tests performed on one sample exposed to 1100°C for 500 hours shows test repeatability is notable. At the same temperature, an increase in toughness with exposure time is highly unlikely which suggests substantial specimen variability.

Table 1,

Temperature (°C)	Exposure Time (hrs)	R (mm)	a (mm)	R/a	Kc (MPa m$^{1/2}$)
as-processed		0	0.27	0.0	5.54
1200	10	1.9	0.29	6.6	0.68
1200	20	3.3	0.33	10.0	0.20
1200	56	3.5	0.34	10.3	0.16
1100	500	1.9	0.28	6.8	0.85
1100	500	1.9	0.28	6.8	0.85
1100	500	1.85	0.31	6.0	1.14
1100	1000	1.1	0.36	3.1	4.22

Microstructural Evaluation

The indent test loads the coating in compression to increase the stored elastic strain energy. As a result, the energy release rate increases above a critical value, the interfacial toughness, for crack propagation. Induced strain from this test is superimposed on the intrinsic strain, from coefficient of thermal expansion (CTE) mismatch, of the TBC and TGO. Two factors that can affect the stored elastic strain energy are total coating thickness and the elastic moduli for the TGO and TBC.

Although the TBC is 100μm thick, channels present between each grain and zirconia's transparency to oxygen ions allow the bond coat to oxidize during thermal exposures. Figure 9 shows the as-processed coating with the thin TGO layer, 250nm, that grows to 2.5μm in 10 hours at 1200°C. From this exposure and keeping the stress state the same, there is a 10 fold increase in the stored elastic strain energy from the TGO.
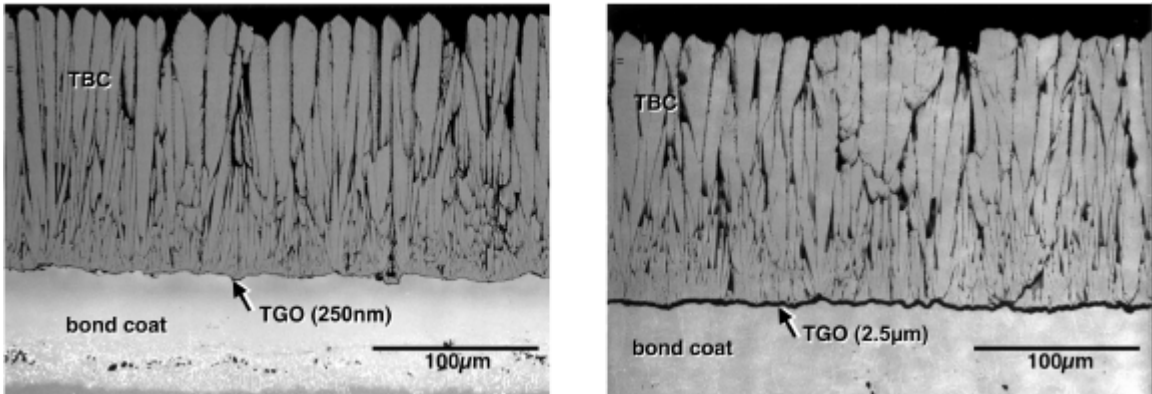
Figure 9. SEM micrograph showing the increase in TGO thickness from the as-processed coating (left image) to the exposed coating (right image).

The TBC contributes to the increase in the stored elastic strain energy by sintering at the high temperatures. Figure 10 shows the disappearance of channels that results in the increase in the effective elastic modulus. Although porosity still lines the original channel location, necks attach grain to grain and reduce the strain tolerance that is appealing to the EBPVD microstructure. This phenomenon is complicated to deal with and is only dealt with in a qualitative manner.
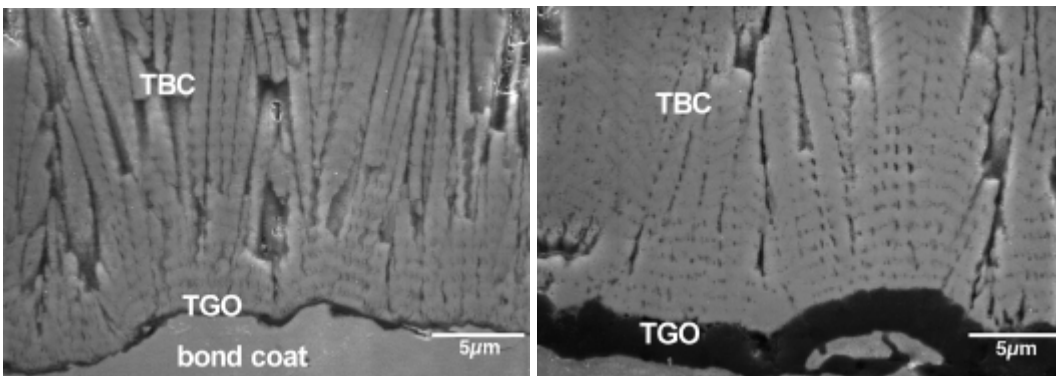

Figure 10. SEM micrograph showing the sintering of the TBC from thermal Exposure. Compare the as-processed coating (left image) with channels between grains and sintered TBC from exposure to 10 hours at 1200°C (right image).

Table 2 shows the toughness results considering the effects of TGO growth and TBC sintering. Here, the mechanisms responsible for the decrease in apparent toughness are separated. Both the TGO growth and TBC sintering increase the driving force for spallation, the stored elastic strain energy. If not considered in the indent test, the decrease in interfacial toughness will be over estimated. These results still represent a drop in the "true" interfacial toughness.

Table 2.

Temperature (°C)	Exposure Time (hrs)	Kc (MPa m$^{1/2}$)			
		Constant Properties	TGO Thickness	TBC Sintering	Both Included
as-processed		5.54	5.54	5.54	5.54
1200	10	0.68	0.81	1.07	1.15
1200	20	0.20	0.26	0.35	0.39
1200	56	0.16	0.23	0.32	0.36
1100	500	0.85	1.61	1.45	1.92
1100	500	0.85	1.61	1.45	1.92
1100	500	1.14	2.07	1.96	2.53
1100	1000	4.22	5.13	8.32	8.81

Oxide Only Systems

Further separation of mechanisms for apparent toughness loss is applying the indent test to the oxide only system. The N5 superalloy with Pt modified aluminide coating was exposed to similar conditions as the TBC system to form an alumina layer. Figure 11 shows the failed regions caused by buckling followed by spallation. Modeling this system is similar to the TBC method except for the absence of the TBC layer with it's contributions to stored elastic strain energy, see Table 3. In Table 3, the right column considers the contributions from alumina growth. There is no significant change in the debond radius, debond size or density of the debonds with exposure time. This could be due to an initiation controlled failure and suggests that the TBC sintering plays an important role in failure.
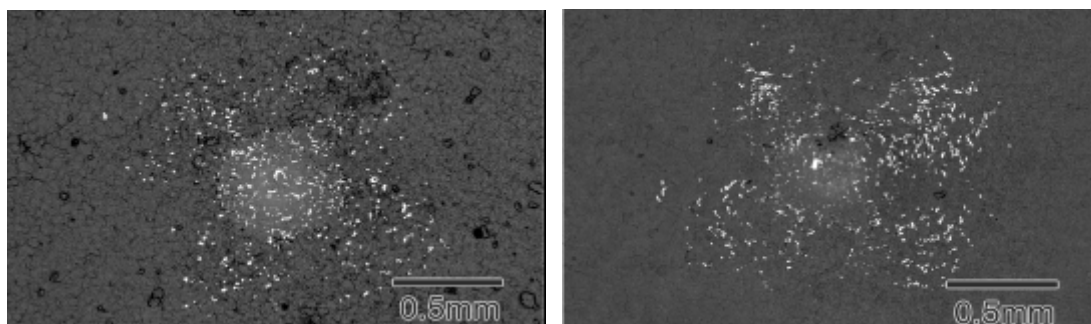

Figure 11. SEM micrographs of the debonded regions (white areas) from the indent test being performed on the bond coat only system. Specmens were exposed to 1200°C for 10 hours (left image) and 56 hours (right image)

Table 3.

Temperature (°C)	Time (hrs)	R (mm)	a (mm)	R/a	Kc (MPa m$^{1/2}$)	
1200	10	0.75	0.28	2.7	1.39	2.76
1200	20	0.78	0.29	2.7	1.39	3.26
1200	56	0.80	0.30	2.7	1.39	4.31
1200	200	0.77	0.30	2.5	1.40	4.78
1200	700	0.85	0.30	3.0	1.36	5.45
1100	100	0.63	0.27	2.3	1.41	2.97
1100	200	0.63	0.29	2.2	1.34	3.42
1100	500	0.66	0.26	2.5	1.40	4.27
1100	1000	0.77	0.34	2.3	1.38	5.33

Summary and Conclusions

The indentation test has proved to be a promising technique for measuring interfacial toughness in TBC systems. This technique has several advantages over other potential techniques. These include

- It is easy to perform with universally available equipment
- It provides physical insight without fracture mechanics
- It can be applied to small specimens
- Bond coat properties are not available
- Incremental loading and multiple indents can yield a significant amount of data from a single specimen.

However, several challenges still remain

- Indent modeling of the substrate is difficult
- Fracture modeling is not complete.

The results obtained to-date with this technique indicate the following

- Significant "apparent" toughness losses are observed from TBC systems exposed at 1100°C and 1200°C
- Increase in TBC thickness and TBC sintering have been found to contribute to coating debonding
- Quantification of the contribution TGO growth and TBC sintering to coating failure still remains to be accomplished
- Preliminary tests with "oxide only" specimens suggest much less loss of interfacial toughness without the TBC present.

Reference

1. M.D. Drory and J.W. Hutchinson, Proc R. Soc. Lond., A., <u>452</u>, 2319, (1996).
2. A. Maricocchi, A. Bartz and D. Wortman (1995). "PVD TBC Experience on GE Aircraft Engines*," Thermal Barrier Coating Workshop*, Proceedings of the Thermal Barrier Coating Workshop, NASA Lewis Research Center, Cleveland, March 27-29, NASA Conference Publication 3312, pp. 79-90, (1995).
3. K.L. Luthra and C.L. Briant. "Mechanism of Adhesion of Alumina on MCrAlY Alloys," Oxidation of Metals, Vol. 26, pp. 397-416, (1986).
4. A.S. Argon, V. Gupta, H.S. Landis and J.A. Cornie "Intrinsic Toughness of Interfaces Between SiC Coatings and Substrates of Si or C Fiber," Journal of Materials Science, Vol. 24, pp. 1207-1218, (1989).
5. R. Stevens, "Engineering Properties of Zirconia" *Engineered Materials Handbook*, ASM International, Vol 4 Ceramics and Glasses, pp. 775-786, (1991).
6. M. Miyayama, K Koumoto, H. Yanagida, "Engineering Properties of Single Oxides" *Engineered Materials Handbook*, ASM International, Vol 4 Ceramics and Glasses, pp. 748-757, (1991).
.